Design of slotless permanent magnet machines by a semi-infinite global optimization method

Zahia Amrouchi, Frédéric Messine, Clément Nadal, Mohand Ouanès

Design of Slotless Permanent Magnet Machines by a Semi-Infinite Global Optimization Method

1st Zahia Amrouchi
LAROMAD, University Mouloud Mammeri
Tizi-Ouzou, Algeria
zahia_amrouchi@yahoo.fr

2nd Frédéric Messine
LAPLACE-CNRS, ENSEEIHT-INPT
Toulouse, France
frederic.messine@laplace.univ-tlse.fr

3rd Clément Nadal
LAPLACE-CNRS, ENSEEIHT-INPT
Toulouse, France
clement.nadal@laplace.univ-tlse.fr

4th Mohand Ouanès
LAROMAD, University Mouloud Mammeri
Tizi-Ouzou, Algeria
ouanes_mohand@yahoo.fr

***Abstract*—An efficient way to design slotless permanent magnet machines is to associate analytical models with deterministic global optimization algorithms. In this paper, we propose to extend these design approaches in order to take into account the torque ripples. This involves the study of a semi-infinite optimization problem. To solve it, a discretization method associated with an exact Branch and Bound global optimization solver is developed. This new approach is validated on some numerical tests showing that efficient global optimal solutions with torque ripples about $5\,\%$ (instead of $30\,\%$) can be so-obtained.**

***Index Terms*—Slotless permanent magnet machines, semi-infinite programming, analytical model, deterministic global optimization.**

I. Introduction

In this work, we address the problem to design a slotless permanent magnet machine (SPMM) when constraints on the torque ripples are taken into account. Starting from an analytical model provided in [1] and [2], an extension is provided here to model the dynamic torque including the torque ripples of such a machine with a three-phase sine wave current supply. Thus, the torque will vary respect to an angle which determines the rotor position. Considering a schedule of conditions, this design problem is formulated as a semi-infinite optimization program. Indeed, the constraints about the torque ripple is said infinite; i.e., it will generate an infinity of constraints depending continuously on the rotor position.

In this work, we will discuss a way to solve this kind of semi-infinite problem by discretizing the angle of the rotor position and by using `COUENNE` a deterministic global optimization solver [3] via the `AMPL` modelling language [4].

In Section II, the analytical model of a SPMM will be presented including its formulation into a semi-infinite program. In Section III, our optimization method is discussed and some numerical results are provided showing that such a method is efficient to design SPMM when constraints on the torque ripples have to be taken into account.

II. Model and Formulation into a Semi-Infinite Optimization Problem

The model of a SPMM provided in [1] has already been designed by deterministic global algorithm [2] and this was improved in [5]. This analytical model only uses the average torque. Herein, a new analytical model is developed to include the torque ripples. The main difference is that harmonics, and their interaction, of the spatio-temporal distributions of stator sine wave currents and rotor square wave magnetic flux density are considered. Some parameters which are now more realistic have been changed from [1], [2] and [5]. This section aims to present the geometry and assumptions leading to an enhanced model taking the torque ripples into account.

A. Geometry and assumptions

The model developed herein concerns an inner-rotor surface-mounted permanent magnet machine without slot. Numerous publications deal with the modelling of such electromechanical converters and propose a simplified sizing approach by considering a few geometric parameters, a required magnetic induction amplitude in the air gap and a net torque to reach as proposed in [1], [2] and [6]. More complex models have been also carried out to predict, for instance, the winding inductances and the armature reaction field of slotless permanent magnet brushless machines [7]. Some authors, like in [8], beside expend great effort in generalizing the calculation of the magnetic field distribution in slotless permanent magnet machines to take into account, for example, eddy currents in conductive regions whose effect is important for the design of very high speed slotless permanent-magnet machines [9]. However, the model addressed herein does not propose to use such general approach but rather a simplified modelling in order to formulate a simple optimization problem.

Thus, the structure considered hereinafter is supposed to be three-phase ($m = 3$) and multipolar (let p be the number of pole pairs). The rotor is composed of $2p$ radially polarized surface-mounted permanent magnets of an angular opening $\theta_a = \beta_a \theta_p$ where $\beta_a \in]0, 1]$ and $\theta_p = \pi/p$ are the magnet

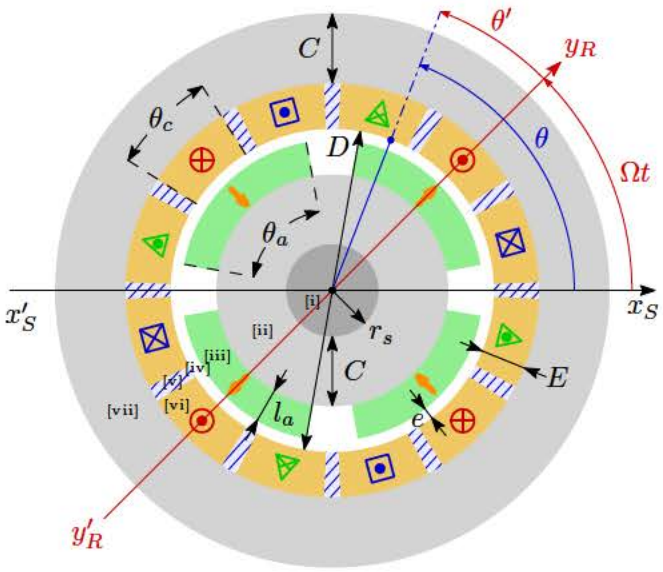

Fig. 1: Simplified geometry of a three-phase four-pole slotless surface-mounted permanent magnet machine ([i] Shaft [ii] Rotor core [iii] Permanent magnet [iv] Mechanical air gap [v] Non-magnetic wedge [vi] Windings [vii] Stator yoke)

angular opening factor and the polar opening angle, respectively. The magnetic induction produced by those magnets in the mechanical air gap is supposed to be purely radial and their relative permeability is considered equal to unity ($\mu_a/\mu_0 = 1$). Concerning the stator, windings are supposed to be reduced to a layer of conductors of a thickness E distributed along the air gap according to a rectangular pattern with an angular opening $\theta_c = \beta_c\theta_p/m$ where $\beta_c \in]0,1]$ is the winding angular opening factor. The geometry is besides supposed to be invariant to axial translations. Lastly, the ferromagnetic parts, namely the stator yoke and rotor core, present a relative permeability much greater than unity ($\mu_{\text{Fe}}/\mu_0 \gg 1$). As an example, a schematic representation of such a structure, that is a three-phase four-pole motor, is pictured in Fig. 1. In this figure, geometric parameters are introduced in order to define the dimensions of the studied machine. They form a part of the variables of the semi-infinite optimization problem collected in Tab. I. In this table, the machine length is considered through the form factor $\lambda = D/L$ defined as the bore diameter D to effective length L ratio.

In addition to those geometric variables, a few input data for the optimization problem are fixed such as the rated net torque Γ_r, the rated speed of rotation N_r or the minimal value of the rotor shaft radius r_s. Furthermore, few magnetic characteristics are set as the magnetic polarization of magnets J_a or saturation magnetic induction of iron parts B_{Fe}. Lastly, the global heating of stator windings is roughly modelled by the quantity E_{ch} equal to the product of the linear current density A_S (defined by the total number of Ampere-turns to the bore perimeter ratio) and the current density in windings J_{Cu}. By using the fill factor k_r, it can be expressed via the following relationship:

TABLE I: Optimization problem variables

Symbol	Definition	Boundaries	Unit
D	Bore diameter	$[10, 500]$	[mm]
E	Winding thickness	$[1, 50]$	[mm]
e	Mechanical air gap	$[1, 5]$	[mm]
l_a	Permanent magnet thickness	$[3, 50]$	[mm]
C	Stator yoke thickness	$[1, 50]$	[mm]
λ	Machine form factor	$[1.0, 2.5]$	[–]
β_a	Magnet angular opening factor	$[0.1, 1.0]$	[–]
B_e	Magnetic induction in the air gap	$[0.1, 1.0]$	[T]
J_{Cu}	Current density in windings	$[10^5, 10^7]$	[A/m^2]
k_f	Magnetic leakage coefficient	$[0.01, 0.30]$	[–]
p	Number of pole pairs	$[\![1, 10]\!]$	[–]

TABLE II: Input data for the optimization problem

Symbol	Definition	Value	Unit
Γ_r	Rated net torque	10.0	[N.m]
N_r	Rated speed of rotation	6000	[rpm]
J_a	Magnetic polarization of magnets	0.9	[T]
B_{Fe}	Saturation magnetic induction of iron	1.5	[T]
E_{ch}	Heating coefficient	10^{11}	[A^2/m^3]
k_r	Fill factor	0.5	[–]
r_s	Minimal shaft radius	10	[mm]
m	Number of phases	3	[–]
β_c	Winding angular opening factor	0.9	[–]

$E_{ch} = A_S J_{\text{Cu}} = k_r E J_{\text{Cu}}^2$. All of the mentioned parameters are gathered in Tab. II.

B. Analytical model

The working principle of a permanent magnet synchronous machine can be seen as the interaction of two travelling waves on the stator bore (at $r = D/2$). According to the simplifying assumptions, the first wave is the square waveform radial component of the magnetic flux density produced by the rotor magnets in motion whose angular distribution $B_{\text{a}}(\theta')$ on a pair pole in the rotor frame is described in Fig. 2. In this figure, $\theta' = \theta - \Omega t$ is the angular position referred to the rotor frame defined from the speed of rotation Ω and angular position θ referred to the stator frame (the axis of the phase 1 is chosen as the stator reference axis). B_e is besides the amplitude of the magnetic induction at the stator bore that can be determined by the consideration of a reluctant circuit between two poles. Thus, it yields:

$$B_e = \frac{2J_a l_a}{D \log\left[\dfrac{D+2E}{D-2(l_a+e)}\right]} \tag{1}$$

where J_a is the magnetic polarization of magnets and log is the natural logarithm.

The second wave is a surface current density wave $k_S(\theta, t)$ highlighting the role of stator windings and the currents

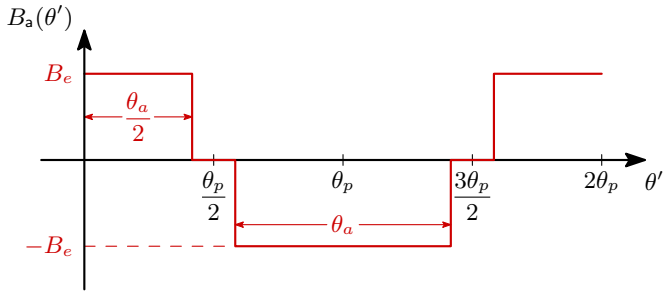

Fig. 2: Angular distribution on a pole pair determined at stator bore of the radial component of the magnetic flux density produced by rotor magnets

flowing in them. This distribution is defined by the sum on the stator phases of products between the space-dependent conductor distribution and the time-dependent current waveform for each phase so much that:

$$k_S(\theta,t)=\sum_{\nu=1}^{m} c_{S\nu}(\theta)i_{S\nu}(t) \tag{2}$$

where $c_{S\nu}(\theta)$ is the conductor distribution of the phase ν whose a representation on a pole pair is pictured in Fig. 3 for all the phases of a three-phase multipolar machine. In this figure, a full pitch single layer winding and conductors of a same phase uniformly distributed on a winding angular opening θ_c are assumed (C_S is the amplitude expressed in conductor/m). Furthermore, $i_{S\nu}(t)$ is the electric current of the phase ν supposed to be sine wave, for the sake of simplicity, so much that:

$$\forall\,\nu\in\{1,\ldots,m\}\,,\; i_{S\nu}(t)=\hat{I}_S\cos\left[\alpha_S(t)-(\nu-1)\frac{2\pi}{m}\right] \tag{3}$$

with $\hat{I}_S$ the current amplitude, $\alpha_S(t)=\omega_S t+\beta_S$ where ω_S and β_S are the electric angular frequency and phase angle, respectively.

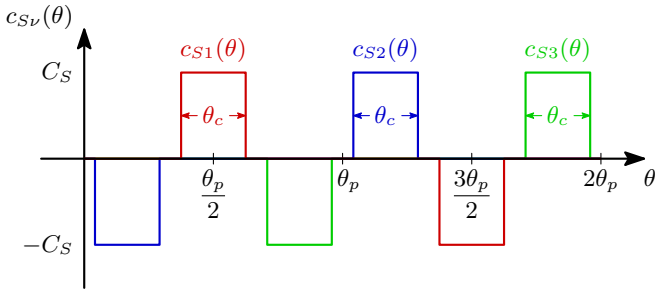

Fig. 3: Conductor distributions on a pole pair for each phase of a three-phase multipolar synchronous machine

Consequently, by applying the Lorentz force on stator conductors and owing to the Newton's third law, the torque exerted on the rotor is defined by the following angular integral such as:

$$\Gamma_{\mathsf{em}}(t)=-p\frac{D^2}{2\lambda}(D+E)\int_0^{\theta_p} k_S(\theta,t)B_{\mathsf{a}}(\theta,t)\mathrm{d}\theta \tag{4}$$

From the definition (2), the waveforms (3) and Fourier series of both distributions drawn in Fig. 2 and Fig. 3, it is possible to compute the previous integral. Hence, under both further conditions of synchronism ($\omega_S=p\Omega$) and maximal torque ($\beta_S=\pi/2$), the dynamic torque (4) is rewritten as follows:

$$\Gamma_{\mathsf{max}}(t)=\langle\Gamma_{\mathsf{max}}\rangle\Big[1+r_\Gamma(t)\Big] \tag{5}$$

where the maximal net torque is:

$$\langle\Gamma_{\mathsf{max}}\rangle=\frac{\pi D^2}{2\lambda}(D+E)\sqrt{2k_rEE_{ch}}\,\mathrm{sinc}\left(\frac{\beta_c\pi}{2m}\right)\cdots \times\beta_aB_e(1-k_f)\,\mathrm{sinc}\left(\frac{\beta_a\pi}{2}\right),$$

where sinc is the unnormalized sine function defined for $x\neq 0$ by $\mathrm{sinc}(x)=\sin(x)/x$ and k_f is a semi-empiric magnetic leakage coefficient. The latter can be expressed only for slotless machines with rectangular waveform surface-mounted permanent magnets by the following formula (see [10], Chap. I, § I.2.2.2, p. 17):

$$k_f=\frac{3}{2}p\beta_a\frac{e+E}{D} \tag{6}$$

The normalized ripples $r_\Gamma(t)$ are also defined as follows:

$$r_\Gamma(t)=\sum_{q=1}^{+\infty}\frac{(-1)^{mq}}{\mathrm{sinc}\left(\frac{\beta_c\pi}{2m}\right)\mathrm{sinc}\left(\frac{\beta_a\pi}{2}\right)}\cos(2mqp\Omega t)\cdots \times\left(\mathrm{sinc}\left[(2mq+1)\frac{\beta_c\pi}{2m}\right]\mathrm{sinc}\left[(2mq+1)\frac{\beta_a\pi}{2}\right]\cdots +\mathrm{sinc}\left[(2mq-1)\frac{\beta_c\pi}{2m}\right]\mathrm{sinc}\left[(2mq-1)\frac{\beta_a\pi}{2}\right]\right).$$

C. Definition of the semi-infinite optimization problem

The eleven variables as well as their variation boundaries of the semi-infinite optimization problem are those gathered in Tab. I. Let denote $\Delta=(D,\lambda,\ldots,p)$ the vector of variables and $S_\Delta=[0.01\,,0.5]\times[1\,,2.5]\times\ldots\times\{1,\ldots,10\}$ the search domain. The idea of this model is to include within a sizing optimization problem based on the minimization of the magnet volume, a continuous, i.e. infinite, constraint which considers a limitation on the torque ripples yielding a semi-infinite program. Here, for simplification purposes, the electric angle $\alpha_e=p\Omega t$ will be used amounting to define the torque ripples

through the new function $\overline{r}_\Gamma(\alpha_e, \Delta) = r_\Gamma(\frac{\alpha_e}{p\Omega}, \Delta)$. Thus, the semi-infinite optimization problem $(\mathcal{P})$ is:

$$(\mathcal{P}) \begin{cases} \min\limits_{\Delta \in S_\Delta} V_m = \pi \beta_a \dfrac{D}{\lambda} l_a (D - 2e - l_a) \times 10^6 \\ u.c. \\ \qquad \langle \Gamma_{\mathsf{max}} \rangle(\Delta) \;=\; \Gamma_r \\ \qquad\qquad E_{ch} = k_r E J_{\mathrm{Cu}}^2 \\ \qquad\qquad B_e = \dfrac{2 J_a l_a}{D \ln\left[\dfrac{D+2E}{D-2(l_a+e)}\right]} \\ \qquad\qquad k_f = \dfrac{3}{2} p \beta_a \dfrac{e+E}{D} \\ \qquad\qquad C = \beta_a \dfrac{\pi D}{4p} \dfrac{B_e}{B_{\mathrm{Fe}}} \\ r_s + C + l_a + e \leq D/2 \\ \qquad |\overline{r}_\Gamma(\alpha_e, \Delta)| \leq l_r \;,\; \forall\, \alpha_e \in [0, 2\pi[\end{cases}$$

where $l_r \in [0, 1]$ is a percentage to limit the torque ripples and V_m is the magnet volume expressed in cm^3. This problem also contains an equality constraint on the thickness C of both stator yoke and rotor core. It can be expressed from the iron magnetic induction B_{Fe} by using Gauss's law for magnetism between the rotor core and a magnet. Note that p is an integer variables and thus, problem $(\mathcal{P})$ is a semi-infinite Mixed-Integer Non-Linear Program (MINLP).

III. Numerical Results of Design

In this approach, to tackle the semi-infinite problem $(\mathcal{P})$, the angle α_e is discretized into n values. This provides $2n$ inequality constraints, which means that $\alpha_e^{[j]} = \frac{2\pi(j-1)}{n}$ with $j \in \{1, \ldots, n\}$. It is a simple efficient way to convert the semi-infinite problem $(\mathcal{P})$ into a MINLP one. Of course, this MINLP is not equivalent to problem $(\mathcal{P})$, it will just numerically approximate it depending on n (the number of discretization steps). Let denote by $(\widetilde{\mathcal{P}}_n)$ this discretization problem deriving from the semi-infinite problem $(\mathcal{P})$In problem $(\widetilde{\mathcal{P}}_n)$, the semi-infinite constraint $|\overline{r}_\Gamma(\alpha_e, \Delta)| \leq l_r, \forall\, \alpha_e \in [0, 2\pi[$ is replaced by the $2n$ inequality constraints $-l_r \leq \overline{r}_\Gamma(\alpha_e^{[j]}, \Delta) \leq l_r, \forall\, j \in \{1, \ldots, n\}$. Remark that increasing n will generate thinner approximations of problem $(\mathcal{P})$. Meanwhile, it will also provide a huge number of inequality constraints which could be difficult to manage by optimization softwares.

In this paper, COUENNE, which is a branch-and-bound based deterministic global optimization MINLP software, is used [3]. COUENNE is carried out via the AMPL environment [4] to describe the discretized problem $(\widetilde{\mathcal{P}}_n)$. In the following, the listings are provided and they present the entire AMPL code; note that these codes are really easy to read and to develop. Indeed, these AMPL codes are quite directly derived from problem $(\widetilde{\mathcal{P}}_n)$; the most difficult parts are the definitions of the constraints about the torque ripples. They are detailed at the end of Listing 1 in the constraints denoted by C_O1 and C_O2 which depends on the set v$= \{1, \cdots, n\}$.

Listing 1: AMPL model of problem $(\widetilde{\mathcal{P}}_n)$: Full_Model.mod

```
# Definitions of the machine parameters
param k_r:=0.5;
param B_Fe:=1.5;
param E_ch:=1e11;
param C_em:=10;
param J_a:=0.9;
param pi:=3.1415926;
param beta_c := 0.9;
param r_s_min := 0.01;

# Variables: bounds and a starting point (for local methods)
var D >=0.01 <=0.5 :=0.01;
var lambda >=1 <=2.5 :=1;
var l_a >=0.003 <=0.05 :=0.003;
var E >=0.001 <=0.05 :=0.001;
var C >=0.001 <=0.05 :=0.001;
var beta_a >=0.1 <=1 :=0.8;
var B_e >=0.1 <=1 :=0.1;
var J_Cu >=1e5 <=1e7 :=1e5;
var k_f >=0.01 <=0.3 :=0.01;
var e >=0.001 <=0.005 :=0.001;
var p >= 1 <=10 :=5  integer;

# function to minimize
minimize Va:pi*beta_a*l_a*(D/lambda)*(D^2*e l_a)*10^6;

# constraints
subject to C1 : C_em = (6*sqrt(2)/(pi*lambda*beta_c))*D^2
                    *B_e*(1 k_f)*(D+E)*sqrt(k_r*E*E_ch)
                    *sin(beta_a*pi/2)*sin(beta_c*pi/6);
subject to C2 : B_e = 2*l_a*J_a/(D
                        *log((D+2*E)/(D^2*l_a 2*e)));
subject to C3 : C = beta_a*B_e*pi*D/(4*B_Fe*p);
subject to C5 : C + l_a + e + r_s_min <= (D/2);
subject to C6 : k_f = (3/2)*p*beta_a*(e+E)/D;
subject to C7 : E_ch = k_r*E*J_Cu^2;
# constraints on the torque ripples
param N_h=5;
set s=1..N_h;
param n=10;
param l_r=0.05;
set v=1..n;
subject to C_O1{j in v} :
      sum{q in s}(1)^(3*q)*( sin((6*q+1)*beta_a*pi/2)
   *sin((6*q+1)*beta_c*pi/6)/((6*q+1)^2*sin(beta_a*pi/2)
   *sin(beta_c*pi/6)) + sin((6*q 1)*beta_a*pi/2)
   *sin((6*q 1)*beta_c*pi/6)/((6*q 1)^2*sin(beta_a*pi/2)
   *sin(beta_c*pi/6)) )*cos(6*q*(2*pi*(j 1)/n)) <=l_r;
subject to C_O2{j in v} :
      sum{q in s}(1)^(3*q)*( sin((6*q+1)*beta*pi/2)
        ... >=l_r;
```

Listing 2: AMPL script for solving problem $(\widetilde{\mathcal{P}}_n)$.

```
reset;
############## Load the model ###############
model Full_Model.mod;

############## Choice of the solver  ########
option solver couenne;
solve; # solve the problem
```

In Tab. III, some results solving problem $(\mathcal{P})$ by approximating it by problem $(\widetilde{\mathcal{P}}_n)$ are presented. In the first row of Tab. III, "w/" or "w/o" denote the fact that torque ripples ("TR") contraints are taken into account or not. For this study, l_r is fixed to $5\,\%$ and the infinite sum to compute $\overline{r}_\Gamma$ is limited to the first five harmonics or the first ten harmonics as mentioned by the value N_h in the second row of Tab. III. The remaining rows in this table are respectively the minimal magnet volume in cm^3, the maximal absolute value of the ripples computed using $n = 360$ discretization steps (1 step by degree) and $N_h = 100$ harmonics (i.e., 100 terms of the sum), the variables corresponding to the optimal solution and

the CPU-time in seconds. Moreover, all the computations are carried out on a MacBook Pro LapTop with a 2.8 GHz Intel Core i7 processor and 16 GB of memory.

TABLE III: Results from the sizing of a slotless permanent magnet machine based on the minimization of magnet volume including a limitation of torque ripples

TR	w/o	w/	w/	w/	w/	w/
(n, N_h)	$\times$	$(10, 5)$	$(18, 5)$	$(50, 5)$	$(100, 5)$	$(100, 10)$
V_m [cm^3]	30.996	51.434	51.649	49.086	49.200	49.460
$\lvert\overline{r}_\Gamma\rvert_{\max}$	0.3314	0.0574	0.0729	0.0574	0.0576	0.0528
D [mm]	290.38	196.35	201.69	191.90	191.58	190.87
E [mm]	4.2048	4.8584	3.2508	4.5678	4.5673	4.5661
e [mm]	1.0000	1.0000	1.0000	1.0000	1.0000	1.0000
l_a [mm]	3.0000	3.0007	3.0000	3.0000	3.0000	3.0000
C [mm]	1.2514	2.2839	1.5027	11.521	11.569	11.676
λ [$-$]	2.5000	2.4999	2.5000	2.5000	2.5000	2.5000
β_a [%]	10.000	36.303	34.534	36.303	36.510	36.980
B_e [T]	0.3292	0.3060	0.3708	0.3159	0.3159	0.3159
J_{Cu} [A/mm^2]	6.8967	6.4160	7.8437	6.6170	6.6173	6.6182
k_f [%]	1.0754	8.1238	9.8255	1.5800	1.5914	1.6176
p [$-$]	4	5	9	1	1	1
Time [s]	366	1232	184	164	358	2663

First, in Tab. III, it can be noticed that if the magnet volume is minimized without taking care about the torque ripples, the optimal design yields a very low magnet volume but with about 33 % of torque ripples. Still according to this table, the branch-and-bound based discretization method addressed herein can find the global optimal design taking into account a limitation on the torque ripples (note that the magnet volume significantly increases). Let remark that when n increases up to 100 (yielding 200 inequality constraints), the CPU-time increases as expected but not so much. Thus, the difficulty to solve the problem $(\widetilde{\mathcal{P}}_n)$ by COUENNE appears to be not so linked to n and it seems to be possible for a branch-and-bound code like COUENNE to manage a great number of constraints (n sufficiently big). Nevertheless, increasing n does not diminish the accuracy on the torque ripples which are about 5.7 % for $n = 10, 50$ and 100. Furthermore, note that when n is a multiple of $2m = 6$ here (stemming from the cosinus in the expression of r_Γ), i.e. $n = 18$ in Tab. III, errors are made on the torque ripples (about 7 %)as proposed in Fig. 5.

An idea to improve the accuracy of such a method is to increase the number of harmonics ($N_h = 10$) taken in sum (see last column in Tab. III). Thus, the maximal torque ripple is now about 5.3 % instead of 5.8 % but this needs a strong computational effort. Moreover, the solution is globally the same; note that the MINLP problem is much more difficult to solve for COUENNE involving the sum of sinus and cosinus and therefore the CPU-time is 7.5 time greater. The differences between the torque ripples are plotted in Fig. 7 and Fig. 8 and it can be seen that the maximum value of the torque ripples is not obtained with 5 harmonics. It is almost reached with 10 harmonics and that makes the differences obtained on the global optimal solutions (see the two last columns of Tab. III). Note finally that using 5 harmonics and $n = 10$ appears to be sufficient to obtain a quite good solutionowing to a point of discretization closely matching a minimal torque value despite an unsatisfactory approximation of torque ripples. Therefore, it appears in Fig. 4 up to Fig. 8 that it is interesting to solve problem $(\widetilde{\mathcal{P}}_n)$ with n sufficiently big ($n = 100$ for example) because, even for $n = 50$, it remains some significant errors (see Fig. 6).

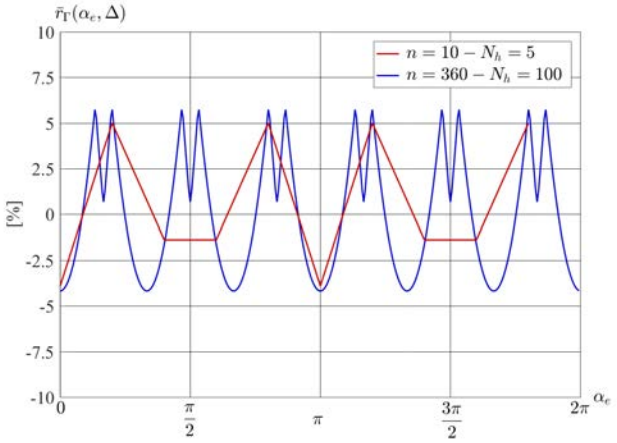

Fig. 4: Torque ripples with $n = 10$ and $N_h = 5$

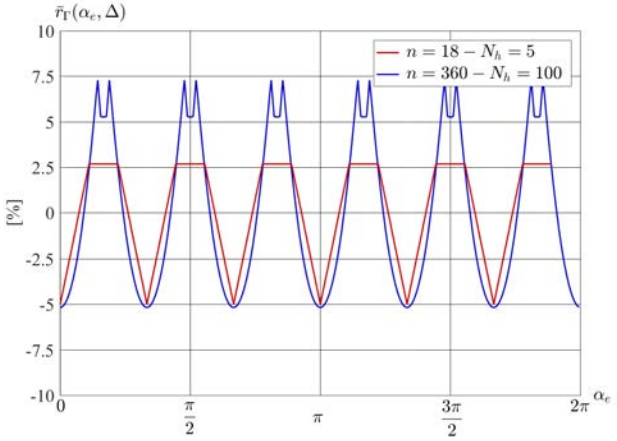

Fig. 5: Torque ripples with $n = 18$ and $N_h = 5$

IV. Conclusion & Discussions

In this paper, a new optimization method is proposed to design SPMM taking into account limitations on the torque ripples. The design method addressed herein is based on the combination of a semi-infinite formulation which uses a SPMM analytical model and a deterministic global optimization MINLP code. The numerical results showed that significant torque ripples can occur in global optimal design solutions (about 33 %) when the torque ripples contraints are not taken into account. Thus, by considering constraints on the torque ripples, this yields global optimal solutions where the torque ripples are strongly reduced (less than 6 %) by using

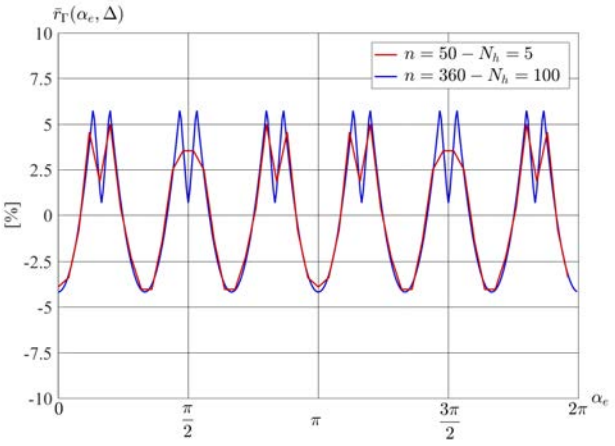

Fig. 6: Torque ripples with $n = 50$ and $N_h = 5$

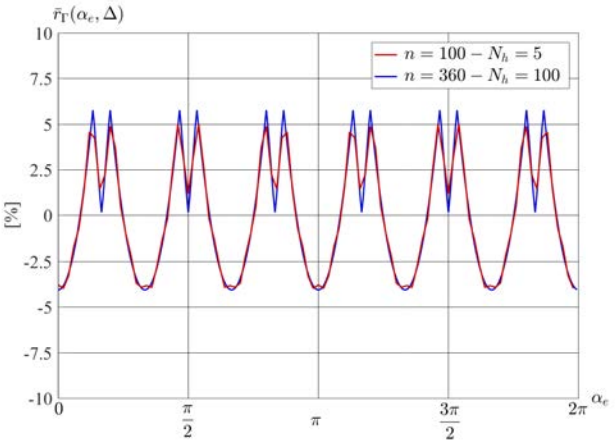

Fig. 7: Torque ripples with $n = 100$ and $N_h = 5$

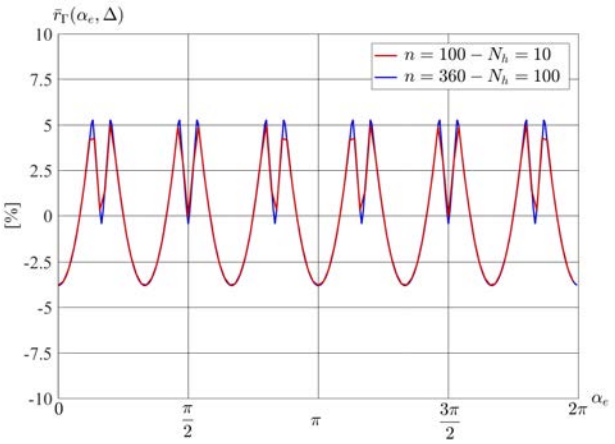

Fig. 8: Torque ripples with $n = 100$ and $N_h = 10$

our discretization method based on `AMPL` and the deterministic MINLP global optimization `COUENNE` solver. This method appears to be particularly efficient in solving those kind of difficult semi-infinite MINLP design problems.

In Listing 2, the `COUENNE` solver is chosen, it could be replaced by another one as `IPOPT` or `SNOPT` which are local solvers. However, these two local solvers cannot take into account the fact that p is an integer variable and they will consider it as a continuous code. In Listing 2, by replacing `couenne` by `ipopt` similar results were obtained mainly with $p = 1$, and by replacing `couenne` by `snopt` no solution is found. Of course these two solvers mainly depends on the starting points provided by the user; see Listing 1. In this study, the optimization routine `fmincon` of `MatLab` was also tested using a multistart based algorithm (with 1000 starting points randomly generated). It appears that only the optimization algorithm based on the interior-point method provides similar results than those presented in Tab. III. Note that the other algorithms `sqp`, `active-set`, `reflective-trust-region` have difficulties to converge. This is mainly due to the fact that using the discretization step to take into account semi-infinite constraints generates a great number of non-linear and non-convex inequality constraints which are difficult to be be considered by `sqp` or `active-set` based optimization algorithms (that is also why `SNOPT` did not work using `AMPL`). It can be noted that the local optimization algorithms based on an interior-point method present some effectiveness in solving those kind of semi-infinite problems using a discretization step. In `MatLab`, it exists a routine `fseminf` which can solve semi-infinite problems such as problem $(\mathcal{P})$. `fseminf` routine works by interpolating (in the iterations of a local optimization solver) the semi-infinite constraints without needing to entirely discretize it. That is an interesting way to solve efficiently semi-infinite NLP by satisfying precisely the semi-infinite constraints (note that in Tab. III, the semi-infinite constraint is always a little bit violated). However, `fseminf` routine is based on a `sqp` based algorithm which appears to never converge to solve problem $(\widetilde{\mathcal{P}}_n)$ and thus, unfortunately `fseminf` routine never converges to a solution.

REFERENCES

[1] B. Nogarède, A.D. Kone, and M. Lajoie-Mazenc, "Optimal Design of Permanent Magnet Machines Using an Analytical Field Modeling", in *Electromotion*, Vol. 2, No. 1, pp. 25-34, 1995.

[2] F. Messine, B. Nogarède, and J.-L. Lagouanelle, "Optimal Design of Electromechanical Actuators: A New Method Based on Global Optimization", in *IEEE Transactions on Magnetics*, Vol. 34, No. 1, pp. 299-307, 1998.

[3] P. Belotti, J. Lee, L. Liberti, F. Margot, and A. Wachter, "Branching and bounds tightening techniques for non-convex MINLP", in *Optimization Methods and Software*, Vol. 24, No. 4-5, pp. 597-634, 2009.

[4] R. Fourer, D. M. Gay, and B. W. Kernighan, *AMPL: A Modeling Language for Mathematical Programming*, Brooks/Cole, 2nd Ed., 2002.

[5] F. Messine, "Deterministic global optimization using interval constraint propagation techniques", in *RAIRO-Operations Research*, Vol. 38, No. 4, pp. 277-293, 2004.

[6] G. R. Slemon, "On the Design of High-Performance Surface-Mounted PM Motors", in *IEEE Transactions on Industry Applications*, Vol. 30, No. 1, pp. 134-140, 1994.

[7] K. Atallah, Z. Q. Zhu, D. Howe, and T. S. Birch, "Armature Reaction Field and Winding Inductances of Slotless Permanent-Magnet Brushless Machines," in *IEEE Transactions on Magnetics*, Vol. 34, No. 5, pp. 3737-3744, 1998.

[8] Z. Q. Zhu, D. Howe and C. C. Chan, "Improved Analytical Model for Predicting the Magnetic Field Distribution in Brushless Permanent-Magnet Machines," in *IEEE Transactions on Magnetics*, Vol. 38, No. 1, pp. 229-238, 2002.

[9] P. Pfister and Y. Perriard, "Slotless Permanent-Magnet Machines: General Analytical Magnetic Field Calculation", in *IEEE Transactions on Magnetics*, Vol. 47, No. 6, pp. 1739-1752, 2011.

[10] B. Nogarède, *Étude de moteurs sans encoches à aimants permanents de forte puissance à basse vitesse*, Thèse de doctorat, Institut National Polytechnique de Toulouse, Toulouse, France, 1990.